Using a Cold Radiometer to Measure Heat Loads and Survey Heat Leaks

M. DiPirro, J. Tuttle, T. Hait, and P. Shirron

Cryogenics and Fluids Branch, NASA/Goddard Space Flight Center, Greenbelt MD 20771 USA

ABSTRACT

We have developed an inexpensive cold radiometer for use in thermal/vacuum chambers to measure heat loads, characterize emissivity and specularity of surfaces and to survey areas to evaluate stray heat loads. We report here the results of two such tests for the James Webb Space Telescope to measure heat loads and effective emissivities of 2 major pieces of optical ground support equipment that will be used in upcoming thermal vacuum testing of the Telescope.

INTRODUCTION

Cold Radiometers

Low cost radiometers were developed to allow in situ measurements of heat flux from both known and unknown sources in thermal-vacuum tests. These radiometers utilize a Winston cone to concentrate incident radiation from a relative compact solid angle onto an absorber and attached thermometer. The absorber and thermometer are weakly coupled to the base of the radiometer on which another thermometer is attached to compare temperatures. The difference between the heated sensor thermometer and the base thermometer, when multiplied by the temperature and gain factor, gives the heat load captured by the radiometer. This, in turn, by knowledge of the emissivity of the absorber and acceptance angle of the Winston cone, gives the equivalent flux emanating from the source. The lower the operating temperature, the more sensitive the thermometers and the better the thermal isolation. The type of thermometers used, Cernox™ 1080, give the best resolution in the 15-25 K range. More details of the design, testing and calibration are given in References 1 and 2. Key features of the radiometers are that the response to signals entering within the angle of acceptance (11° half angle field of view (FOV)) is flat and the absorbing material, "Steelcast" is wavelength independent [3] over the blackbody radiation spectrum of interest in these tests. These properties greatly simplify the calibration and interpretation of the radiometer signals.

The radiometers can be calibrated in situ by applying extra electrical power to the thermometer and reading out the apparent temperature. The same is done for the base thermometer to compensate for the self-heating within the sensor itself. A plot of input power vs. temperature difference between the sensor and the base then produces the gain of the radiometer.

JWST Testing

The James Webb Space Telescope (JWST) is a 6.7 m diameter visible and infrared telescope that will be operated in the 40-60 K range in space. To verify proper operation, the telescope and instruments will be tested in large thermal-vacuum chambers. These tests are very expensive, so to reduce risk, several pieces of critical Ground Support Equipment (GSE) to be used for these tests are characterized for optical and thermal performance. The radiometer-related aspects of two of these GSE thermal tests will be described in this paper. A third major piece of optical GSE, the Cryogenic Photogrammetry Module was also tested using cold radiometers. Results of that test will be reported later.

COCOA TESTS

One of the pieces of critical GSE is the Center of Curvature Optical Assembly (CoCOA). This large interferometer operates outside the thermal vacuum chamber at room temperature but has a view into the chamber through a large glass port. To protect thermal balance testing, a passively cooled shutter is placed in front of the window when the CoCOA is not being used. It was necessary to measure the shutter temperature and thermal emissivity and the emission from the CoCOA itself in two configurations with the shutter open.

A test of the CoCOA was performed at Marshall Space Flight Center's large 20 K-shrouded thermal vacuum chamber know as the XRCF. While the CoCOA itself was within a surrounding 120 K shroud, it operates at room temperature and in normal room temperature air. It was therefore surrounded by a hermetic shell and by MLI and kept warm by the flow of air ducted from outside the chamber. A plate cooled by a dedicated 20 K refrigerator cryogen loop was mounted directly under the CoCOA. Four radiometers were placed on this plate as shown in Fig [xx] under the CoCOA shutter. The radiometers had an additional cylinder surrounding the Winston cone to prevent stray radiation from a warm (120 K) part of the shroud from heating the body of the radiometer. An additional radiometer was positioned on the cold plate to look directly at this hot part of the shroud.

The shutter was constructed with an aluminum frame with an MLI blanket. It was thermally isolated from the room temperature CoCOA and was allowed to float thermally between the warm CoCOA above and the cold chamber below. On the bottom of the shutter, the last, outward facing layer was black kapton with VDA aluminum on the blanket side. It was this layer that the radiometers faced. Radiometer #4, R4, faced the the center of this outer blanket. A Cernox thermometer was taped to the outside of the blanket and covered with a small patch of black kapton to match the emissivity of the rest of the shutter. By measuring the temperature the radiometer reading could be converted directly to an effective emissivity.

The shutter was allowed to cool to its equilibrium temperature over several days. The cold plate below the shutter was maintained at less than 24 K during this time. Radiometer measurements were made continuously. All 4 radiometers viewing the shutter game the same reading to within 5%. The shutter temperature reached 103.4 K and from the R4 reading its emissivity was 0.62 which is slightly lower than the expected value of 0.74 at this temperature. Perhaps the aluminized surface provided a reflection of any transmitted radiation. The total emission per area from the shutter bottom surface was 4000 mW/m^2, which, in turn is used to calculate the amount of power escaping into the chamber to be 0.27 W, which is within the acceptable range for its final use in the JWST test.

The shutter was then opened. Two modes of the CoCOA with different thermal signatures were tested: one with a hologram in place which has blanketing limiting the total heat output, and one with the hologram retracted which had the signature of a 293 K blackbody. For this mode the heat load out of the aperture was 27.8 W.

These tests were repeated several times for different durations over several weeks to simulate expected operations in Chamber A and to test the thermal limits and transient response.

The radiometers were not initially designed to stare at a heat source as large as room temperature over the entire FOV. To obtain accurate results when the radiometer was operated with a very high heat load, it was necessary to calibrate the same radiometer a second time in the presence of this high heat load. The same calibration procedure as performed at low temperature was followed, but higher electrical power was used. The temperature-dependence curve that was used for readout between 15

and 25 K was surprisingly relatively accurate even when the sensing element was at 75 K, and followed the thermal conductance dependence of stainless steel as expected. This gave confidence in the accuracy of the heat load measurements.

OSIM TESTS

Objectives

Before integrating the Integrated Science Instrument Module (ISIM) to the telescope, ISIM is tested by itself in a smaller thermal-vacuum chamber at Goddard Space Flight Center (GSFC). A smaller, simulator telescope, the Optical Simulator for the Instrument Module (OSIM) is used to test the instruments. OSIM was cryogenically tested before installation of ISIM, characterizing its optical and thermal performance. The thermal performance tests included a measurement of the heat load into ISIM (nominal 40 K) from OSIM (nominal 100 K). Compared to the JWST primary, secondary and tertiary mirrors, OSIM emits a significant amount of heat --100 K vs. 30-50 K for the flight mirrors. An important measurement to be made in the ISIM test is the lead load balance; measure heat into ISIM through harnesses, structure and internal dissipation to determine if the passive radiators have sufficient cooling power to maintain the instruments at their operating temperature (typically 36-40 K). To limit the amount of heat entering the ISIM cavity from OSIM a baffle is used. The baffle is a slightly tapered, rectangular cross section, duct whose inside is painted with Ball InfraRed Black (BIRB) which has a high emissivity and low specularity.

The goals of the radiometer measurements were to measure the heat load that will radiate from the OSIM into the ISIM cavity, determine the effectiveness of the baffle in limiting this heat load, and determine the effective emissivity of the OSIM aperture.

Set Up

Six radiometers were stationary, positioned around the exit aperture two of which had a view of only the upper portion of the baffle and four of which had views of the four walls of the baffle. None of these radiometers had a view of the lowest 20% of the baffle or the aperture. Two radiometers were attached to a moveable stage that translated across the baffle, aperture, and a support structure. These two radiometers pointed directly down. (See Figures 3 and 4.) Unfortunately all radiometers but the lowest two were mounted to structures that were not well anchored to the 15 K shroud, and due to dissipation by the optical GSE attached to the moveable structure, operated at temperatures between 34-47 K for the first test, and 29-36 K in the second test. This highest temperatures had two adverse effects: It limited the resolution (signal to noise) of the radiometers, and caused a longer that expected time constant of 5-10 minutes rather than the expected 10-20 seconds. Part of this linger time constant was due to the structure itself relaxing rather than the radiometer. Heat from the optical instrument also appeared as a reflection off some of the neighboring surfaces visible to the radiometer, which confused the results. The two radiometers viewing only the very upper portion of the baffle were properly anchored at 17 K and had excellent signal to noise. These demonstrated that no noticeable reflections (< 5 mW/m^2) came from the upper baffle.

Results and Analysis

The measurements performed on the OSIM suffered from the number of different thermal emitters in the field of view. When the radiometer is centered over the aperture the view is represented by the schematic in Fig. 5. Interpretation of this scene is ambiguous. To help deconvolve the radiation coming from each of the sources, the radiometer was translated across the exit of the aperture in the direction indicated in Fig 6. Near the edge of the baffle the change in signal was greatest, so the radiometer was moved in 25 mm steps. We compare the proportion of the FOV of each of the items multiplied by a flux per unit area for each item to come up with a predicted value for the flux into the radiometer. This result is compared to the actual reading. A best fit to the data is obtained by varying

each of the items' flux intensity. The result of this analysis is shown in Fig 7. Once the flux intensity is obtained, the heat load is determined by multiplying by each item's view factor. A more thorough analysis of the view factors will be done in the future to better fit the measured values.

For OSIM we obtained a total heat load of 20.6 mW ± 2.0 mW through the exit of the baffle. This consists of 17 mW from the entrance aperture to the baffle, 0.1 mW from the mirror chain, and 3.5 mW from reflections from the baffle, primarily from the area near the entrance aperture. The primary contributors to the error bar are uncertainty in the location of baffle reflections and MATF reflections, and the absolute accuracy of the radiometer calibration.

SUMMARY

This paper describes two tests using the cold radiometers developed at NASA. The results demonstrate the usefulness of the radiometers in determining radiative heat fluxes, and effective emissivities. Even when a scene has several different emitters within it, by varying the radiometer position and/or the temperature of the sources, knowledge of the flux from each item can be obtained.

REFERENCES

1. DiPirro, M., Hait, T., Tuttle J., and Canavan, E., "A low cost, low temperature radiometer for thermal measurements", Proc. SPIE 7439C-44 (2009).
2. DiPirro, M., Tuttle, J., Canavan, E., and Shirron, P., "Use of Cold Radiometers in Several Thermal/Vacuum Tests", Adv. Cryo. Eng. 57, (2012) pp. 1513-1518.
3. E. J. Wollack, D. J. Fixsen, R. Henry, A. Kogut, M. Limon, and P. Mirel, "Electromagnetic and Thermal Properties of a Conductively Loaded Epoxy", Int. J. Infrared and Millimeter Waves (2008) 29:51-61.

FIGURES

See the following pages.

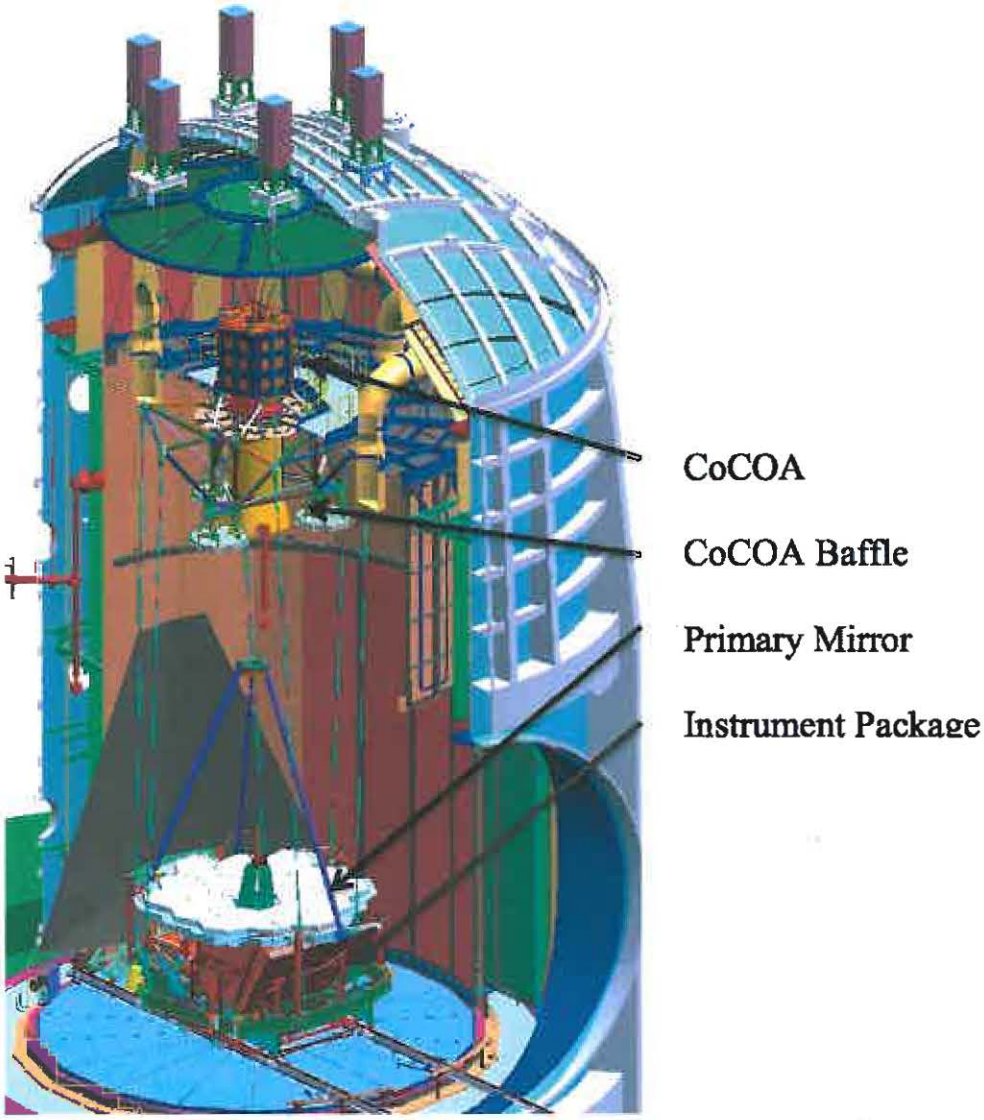

Fig. 1. Test configuration of the JWST telescope and instrument package at Johnson Space Flight Center, Chamber A

Fig. 2. Four radiometers (R4 is back center) mounted on the cold plate under the CoCOA shutter. The shutter has a "U" shaped opening for balancing and is in the open position in this picture.

Fig. 3. Three dimensional drawing of the OSIM test apparatus, showing the baffle (blue and red) and FOVs of the fixed radiometers (gray cones). The radiometers' central axes are shown as red lines. The vertical red lines are from the two translating radiometers.

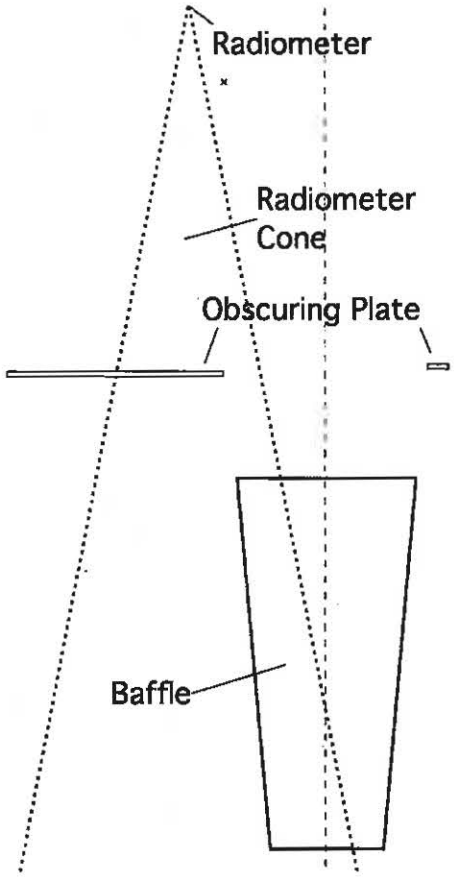

Fig. 4. A schematic elevation of the baffle, obscuring plate, and radiometers. The radiometer cone is 11° half angle. The radiometer position shown is 320 mm to the left of the center position.

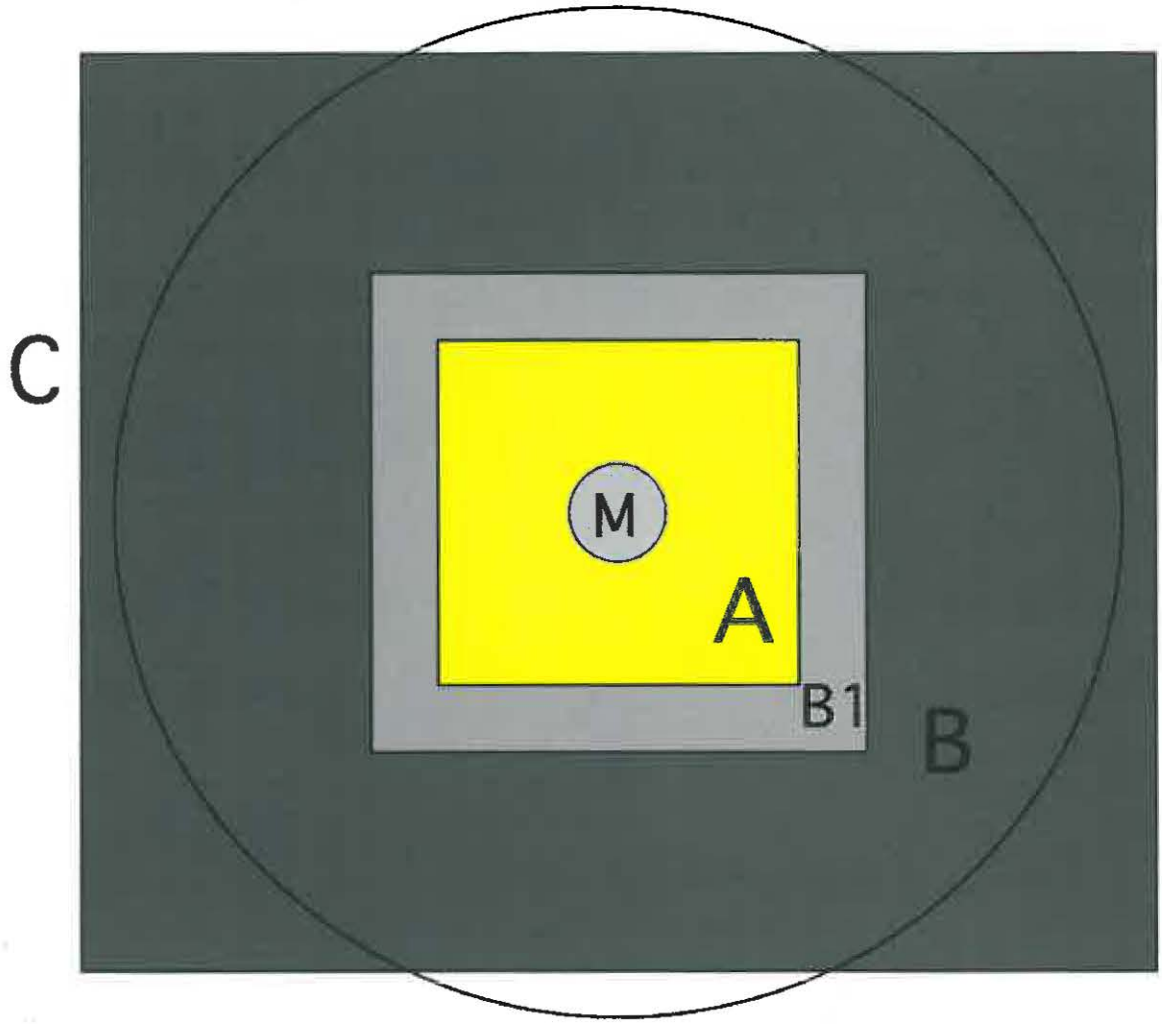

Fig. 5. Depiction of the scene within the radiometer FOV. Area A is the aperture to the OSIM mirror chain, M is the mirror chain, B is the upper 80% of the baffle, B1 is the lower 20% of the baffle, and C is the MATF, the plate above the exit of the baffle. The circle is the radiometer field of view.

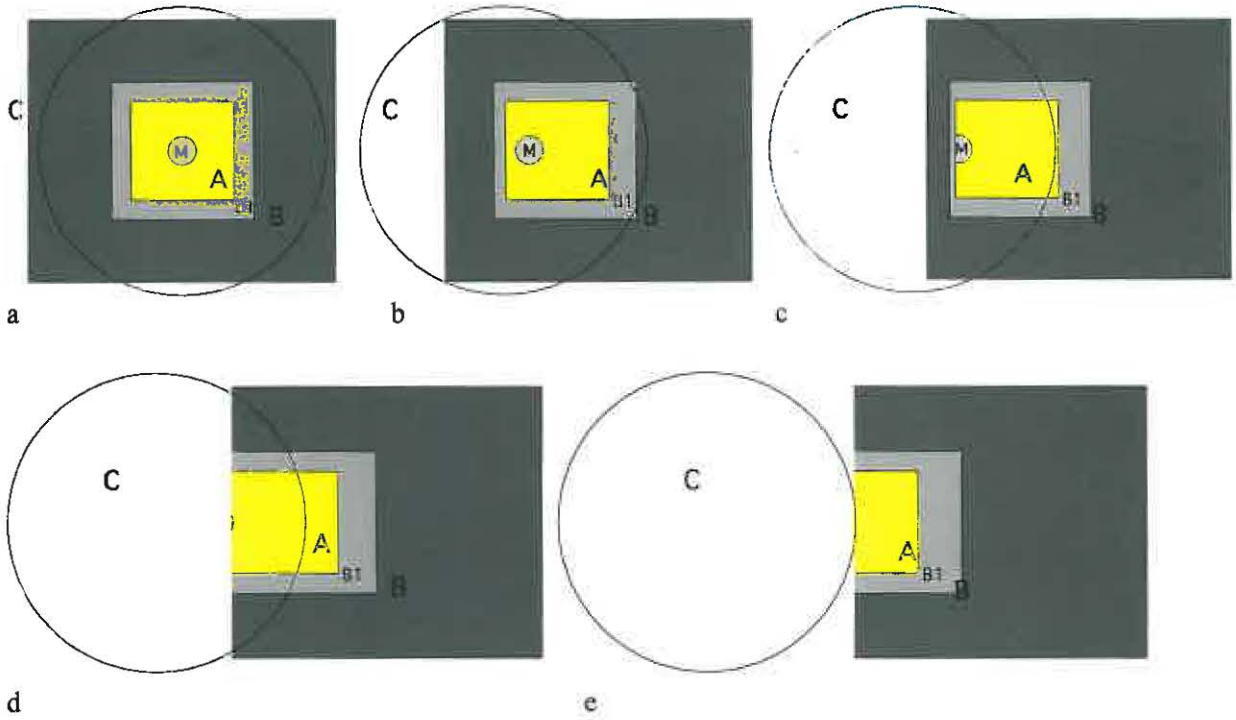

Fig. 6. Progression of the FOV as the radiometer translates from the center to the left side of the baffle and aperture. A=centered, b=140 mm left, c=223 mm left, d=323 mm left, e= 398 mm left. Note that items moving to the right are in the foreground and items moving to the left are in the background relative to the center of the entrance aperture, A.

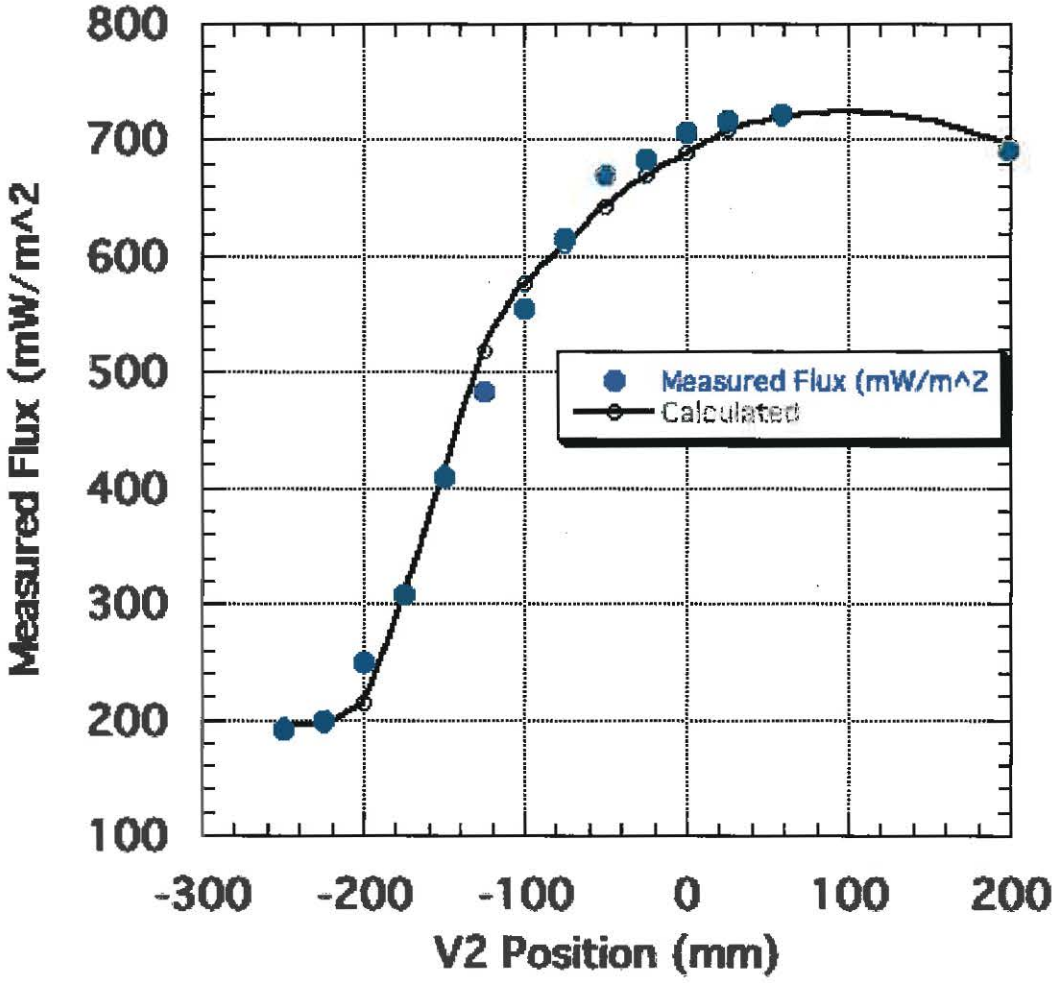

Fig. 7. The radiometer measurements and calculated results for OSIM. Note that the line is a guide to the eye for the calculated values and not a fit to the data. The error bars on the measurements are approximately the size of the filled circles.